References and Notes

1. B. Bukau, E. Deuerling, C. Pfund, E. A. Craig, *Cell* **101**, 119 (2000).
2. B. Bukau, A. L. Horwich, *Cell* **92**, 351 (1998).
3. F. U. Hartl, *Nature* **381**, 571 (1996).
4. D. R. Palleros, K. L. Reid, L. Shi, W. J. Welch, A. L. Fink, *Nature* **365**, 664 (1993).
5. M. Pellecchia *et al.*, *Nature Struct. Biol.* **7**, 298 (2000).
6. G. C. Flynn T. G. Chappell, J. E. Rothman, *Science* **245**, 385 (1989).
7. D. M. Cyr, X. Lu, M. G. Douglas, *J. Biol. Chem.* **267**, 20927 (1992).
8. J. S. McCarty, A. Buchberger, J. Reinstein, B. Bukau, *J. Mol. Biol.* **249**, 126 (1995).
9. K. Liberek, D. Skowyra, M. Zylicz, C. Johnson, C. Georgopoulos, *Proc. Natl. Acad. Sci. U.S.A.* **88**, 2874 (1991).
10. L. Packschies *et al.*, *Biochemistry* **36**, 3417 (1997).
11. A. Szabo *et al.*, *Proc. Natl. Acad. Sci. U.S.A.* **91**, 10345 (1994).
12. C. J. Harrison, M. Hayer-Hartl, M. Di Liberto, F.-U. Hartl, J. Kuriyan, *Science* **276**, 431 (1997).
13. J. Höhfeld, S. Jentsch, *EMBO J.* **16**, 6209 (1997).
14. S. Takayama *et al.*, *Cell* **80**, 279 (1995).
15. S. Takayama *et al.*, *EMBO J.* **16**, 4887 (1997).
16. M. Zeiner, M. Gebauer, U. Gehring, *EMBO J.* **16**, 5483 (1997).
17. H.-G. Wang, S. Takayama, U. R. Rapp, J. C. Reed, *Proc. Natl. Acad. Sci. U.S.A.* **93**, 7063 (1996).
18. A. Bardelli *et al.*, *EMBO J.* **15**, 6205 (1996).
19. R. Liu *et al.*, *J. Biol. Chem.* **273**, 16985 (1998).
20. J. Lüders, J. Demand, J. Höhfeld, *J. Biol. Chem.* **275**, 4613 (2000).
21. S. Takayama, Z. Xie, J. C. Reed, *J. Biol. Chem.* **274**, 781 (1999).
22. D. Bimston *et al.*, *EMBO J.* **17**, 6871 (1998).
23. Supplemental Web material is available at www.sciencemag.org/cgi/content/full/291/5508/1553/DC1.
24. J. K. Stuart *et al.*, *J. Biol. Chem.* **273**, 22506 (1998).
25. We determined ATP hydrolysis rates as described (*9*), using 3 μM Hsc70 purified from bovine brain in the presence or absence of 3 μM Hsp40, Bag-1M, or Bag domain, as indicated in Fig. 1C.
26. Hsc70 release from substrate was measured as described (*33*).
27. Bovine Hsc70 ATPase (residues 5–381, identical to the human homolog) and Bag domain (residues 151–363 of human Bag-1M) were produced as His^6-tagged proteins in *E. coli*. A selenomethionine (Se-Met)-labeled derivative of the ATPase domain was produced in the *E. coli* strain B834(DE3). After chromatography on NiNTA (Qiagen, Valencia, CA), the His^6-tag of the Bag domain was removed by using tobacco etch virus (TEV) protease. A stable, nucleotide-free complex with a 1:1 stoichiometry [see Web table 1 (*23*)] was purified to homogeneity by chromatography on Resource Q (Pharmacia), followed by gel filtration. Crystals were grown at 20°C in hanging drops by mixing equal volumes of protein complex [40 mg/ml in 10 mM Hepes (pH 7.5)] and reservoir solution [50 to 100 mM K-Na-tartrate, 12 to 16% polyethylene glycol (average molecular weight of 3350), 0.1 M tris (pH 8.5), and 25% (w/v) glycerol]. Crystals were flash-cooled in liquid nitrogen and kept at 100 K during data collection at beamlines ID14-4 [European Synchrotron Radiation Facility (ESRF), Grenoble, France], for native data, and BW6B [Deutsches Elektronen-Synchrotron (DESY), Hamburg, Germany], for multiple anomalous dispersion (MAD) data. Data sets were processed with the HKL software package (*34*). Structure solution was achieved by MAD phasing techniques with the program SOLVE (*35*). After solvent correction with the program DM (*36*), the known structure of the ATPase domain of Hsc70 was placed into the electron density, and the structure of the Bag domain was built manually. The structure was refined with the program CNS (*37*). The somewhat high R_{free} of the final model can in part be attributed to significant radiation damage during the collection of the native data set that could only be partially corrected during data processing and scaling. The His^6 tag of the Hsc70 ATPase was completely disordered and is not included in the final model. Upon crystallization, a disulfide bridge between Cys^{259} at the COOH-terminus of the Bag domain and Cys^{201} was formed. However, binding of the Bag domain to Hsc70 was not affected by reducing agents.
28. H. Sondermann, unpublished data.
29. K. M. Flaherty, C. DeLuca-Flaherty, D. B. McKay, *Nature* **346**, 623 (1990).
30. J.-H. Ha, D. B. McKay, *Biochemistry* **34**, 11635 (1995).
31. H. Theyssen, H. P. Schuster, L. Packschies, B. Bukau, J. Reinstein, *J. Mol. Biol.* **263**, 657 (1996).
32. P. A. Boriack-Sjodin, S. M. Margarit, D. Bar-Sagi, J. Kuriyan, *Nature* **394**, 337 (1998).
33. J. C. Young, F. U. Hartl, *EMBO J.* **19**, 5930 (2000).
34. Z. Otwinowski, W. Minor, *Methods Enzymol.* **276**, 307 (1997).
35. T. C. Terwilliger, J. Berendzen, *Acta Crystallogr.* **D55**, 849 (1999).
36. Collaborative Computational Project Number 4, *Acta Crystallogr.* **D50**, 760 (1994).
37. A. T. Brünger *et al.*, *Acta Crystallogr.* **D54**, 905 (1998).
38. R. M. Esnouf, *Acta Crystallogr.* **D55**, 938 (1999).
39. A. Nicholls, R. Bharadwaj, B. Honig, *Biophys. J.* **64**, A166 (1993).
40. A. C. Wallace, R. A. Laskowski, J. M. Thornton, *Protein Eng.* **8**, 127 (1995).
41. Single-letter abbreviations for the amino acid residues are as follows: A, Ala; C, Cys; D, Asp; E, Glu; F, Phe; G, Gly; H, His; I, Ile; K, Lys; L, Leu; M, Met; N, Asn; P, Pro; Q, Gln; R, Arg; S, Ser; T, Thr; V, Val; W, Trp; and Y, Tyr.

42. We thank M. Rosenhagen for help with protein crystallization and the staff at the European Molecular Biology Laboratory and Max-Planck-Institut beamlines for their support during data collection. J.H. was supported by the Deutsche Forschungsgemeinschaft (grant Hö 1518/4-1). Protein coordinates are available from the Protein Data Bank (PDB) (code 1HX1).

8 November 2000; accepted 17 January 2001

Taste Receptor Cells That Discriminate Between Bitter Stimuli

Alejandro Caicedo[1,3]* and Stephen D. Roper[1,2,4]

Recent studies showing that single taste bud cells express multiple bitter taste receptors have reignited a long-standing controversy over whether single gustatory receptor cells respond selectively or broadly to tastants. We examined calcium responses of rat taste receptor cells in situ to a panel of bitter compounds to determine whether individual cells distinguish between bitter stimuli. Most bitter-responsive taste cells were activated by only one out of five compounds tested. In taste cells that responded to multiple stimuli, there were no significant associations between any two stimuli. Bitter sensation does not appear to occur through the activation of a homogeneous population of broadly tuned bitter-sensitive taste cells. Instead, different bitter stimuli may activate different subpopulations of bitter-sensitive taste cells.

Recently, a large family of bitter taste receptors was identified in humans and rodents (*1, 2*). Although individual receptors were shown to respond selectively to a particular compound (*3*), taste cells expressed mRNAs for several receptors (*1, 2*). The findings were interpreted as showing that individual taste cells respond to several different compounds (*1*). However, behavioral and physiological studies in humans, monkeys, and rats indicate that bitter stimuli can be discriminated (*4–8*). Whether taste cells respond specifically to certain bitter stimuli is an unresolved issue. Unfortunately, our understanding of whether taste cells respond to multiple bitter compounds has depended on inferences from indirect studies [expression patterns of receptor mRNA (*1, 2*) and recordings from the afferent nerve (*7*) and cortical neurons (*8*)]. Here, we used Ca^{2+} imaging to measure direct activation of taste cells in situ to investigate how bitter taste stimuli are detected in taste buds (*9*). With this method, it is possible to view single taste cells in foliate slices in situ with a confocal microscope and record Ca^{2+} changes in intact taste buds (*9–11*) (Fig. 1). A series of representative compounds widely used in studies of bitter taste was selected for this study at concentrations that elicit behavioral responses in rats (*12–20*).

Cycloheximide (10 μM) induced large transient intracellular Ca^{2+} increases in foliate taste cells that showed little if any adaptation or desensitization [mean peak amplitude of the relative fluorescence change $\Delta F/F$, 46.6 ± 6.5% (Fig. 2)]. This contrasts with the pronounced adaptation reported for the expressed murine cycloheximide receptor (*3*). Lowering extracellular Ca^{2+} concentration did not reduce cycloheximide responses in the cell bodies (Fig. 2D) (*21*) or apical processes. None of the cells that responded to cycloheximide

[1]Department of Physiology and Biophysics, [2]Program in Neuroscience, University of Miami School of Medicine, 1600 NW 10th Avenue, Miami, FL 33136, USA. [3]Laboratorio de Biofísica, Centro Internacional de Física, AA 49480, Bogotá, Colombia. [4]Rocky Mountain Taste and Smell Center, Denver, CO 90262, USA.

*To whom correspondence should be addressed. E-mail: acaicedo@chroma.med.miami.edu

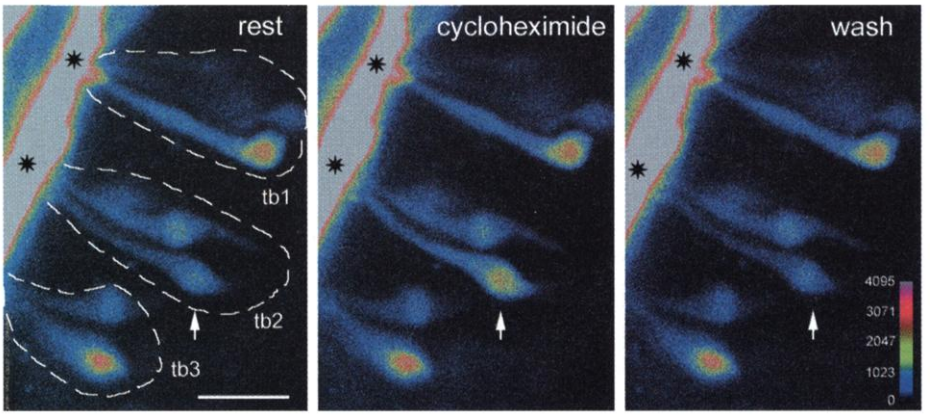

Fig. 1. Ca^{2+} response to the bitter compound cycloheximide (10 μM). Three sequential confocal images of a lingual slice showing individual taste cells loaded with CaGD in adjacent foliate taste buds (outlined, tb1 to tb3). Only one cell (arrow) responds to the stimulus. Apical processes extend to and converge at the taste pore (asterisks). Scale bar, 20 μm. Color palette shows the intensity mapping (range, 0 to 4095; 12-bit data).

(n = 16) responded to depolarization with 50 mM KCl, although neighboring cells did (*9*). Thus, cycloheximide-induced Ca^{2+} signals did not appear to depend on Ca^{2+} influx through voltage-gated Ca^{2+} channels (*22*). Our results are consistent with studies showing that other bitter stimuli raise inositol trisphosphate levels and release Ca^{2+} from intracellular stores (*23–26*).

The other bitter stimuli that we tested induced smaller Ca^{2+} responses [mean peak amplitudes from 5.1 to 12.5% (Fig. 3A)]. In contrast to cycloheximide, denatonium, and quinine, sucrose octaacetate (SOA) and phenylthiocarbamide (PTC) responses were prolonged [up to several minutes (Fig. 3B)]. Responses to the five compounds tested showed concentration dependency and had different activation thresholds (Fig. 3C). The response thresholds for all five stimuli were strikingly similar to the behavioral thresholds in rats (*27*).

Only 18% of all cells tested (69 out of 374) showed responses to one or more of the test compounds when applied at or slightly above midrange concentrations (Fig. 3C). Responses to the compounds were observed in the percentage of taste cells as follows: cycloheximide (10 μM), 14% of the taste cells (51 out of 374); quinine (300 μM), 4.5% (17 out of 374); denatonium (100 μM), 3.7% (14 out of 374); PTC (300 μM), 2.4% (9 out of 374); and SOA (500 μM), 1.6% (6 out of 374). The low incidence of the denatonium responses corresponds well with previous observations on rat taste buds (*25, 28*). The proportion of bitter-responsive cells per taste bud (average, 17.6 ± 2.8%) was similar to the proportion of bitter-sensitive cells within the entire taste cell population

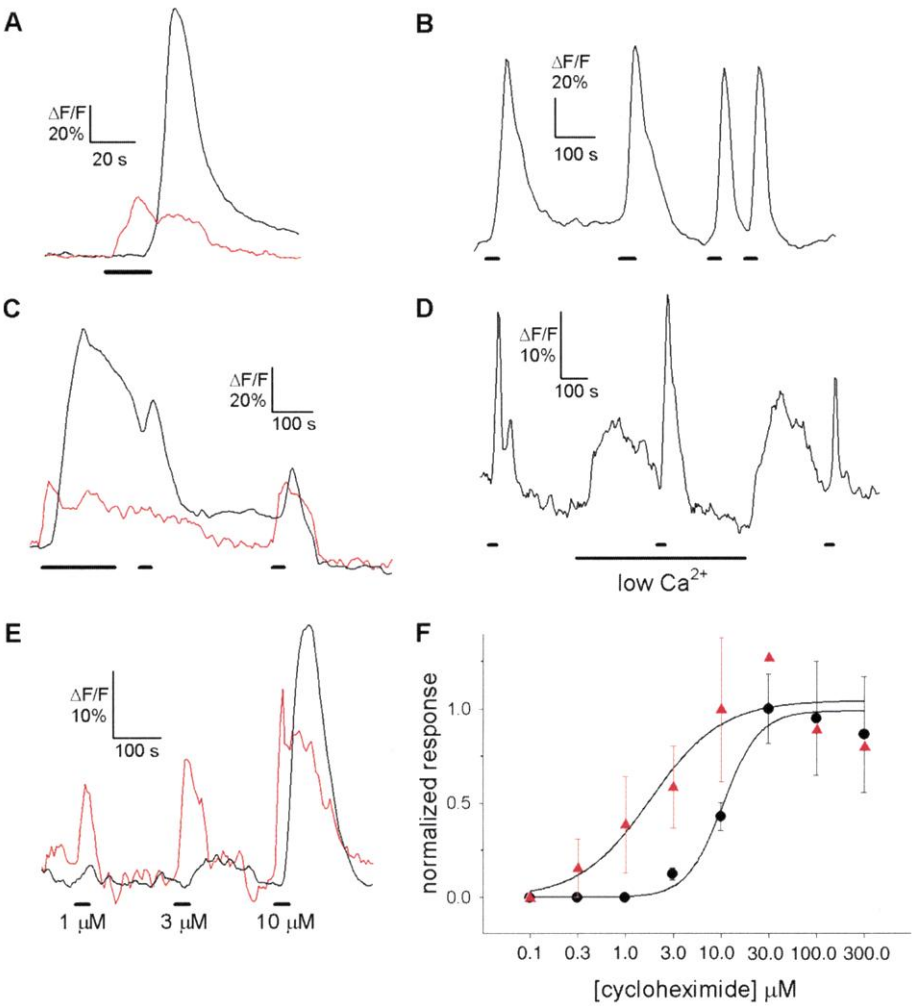

Fig. 2. Cycloheximide-induced Ca^{2+} responses in single taste cells. (**A**) The Ca^{2+} response to cycloheximide (10 μM) appears 20 s earlier in the apical tip (red trace) than in the cell body (black trace) of the same taste cell. There is a secondary Ca^{2+} increase in the apical process that is coincident with the larger Ca^{2+} transient in the cell body. This may represent diffusion of Ca^{2+} from the cell body (i.e., backflow). Bars under traces denote the application of taste stimuli in (A) through (E). (**B**) Repetitive stimulation with cycloheximide did not decrease the amplitude of the response. (**C**) Prolonged application of cycloheximide (10 μM) resulted in only a small decline in response (adaptation) in the apical tip (red trace) and cell body (black trace), which may be due to depletion of the intracellular Ca^{2+} stores. (**D**) Cycloheximide responses were not abolished by lowering the Ca^{2+} concentration in the bath solution to a nominal 0 mM. Changing the Ca^{2+} concentration in the bath solution induced changes in intracellular Ca^{2+} (*21*). (**E**) Concentration dependency of cycloheximide-induced Ca^{2+} responses in the apical tip (red trace) and the cell body (black trace). The apical tip was more sensitive than the cell body. The differences in sensitivity and time course of the responses between the apical process and the cell body suggest that these regions constitute distinct physiological compartments, as reported for olfactory receptor neurons (*30*). (**F**) Concentration-response relations for peak responses to cycloheximide in the apical process (red triangles) (n = 5 taste cells) and the cell body (black circles) (n = 9). Not all concentrations could be tested in every cell. Responses were normalized to the average response at 10 μM (apical process) and 30 μM (cell bodies). Data were curve-fitted with SigmaPlot 5.0 (SPSS, Chicago, Illinois). Error bars indicate SEM.

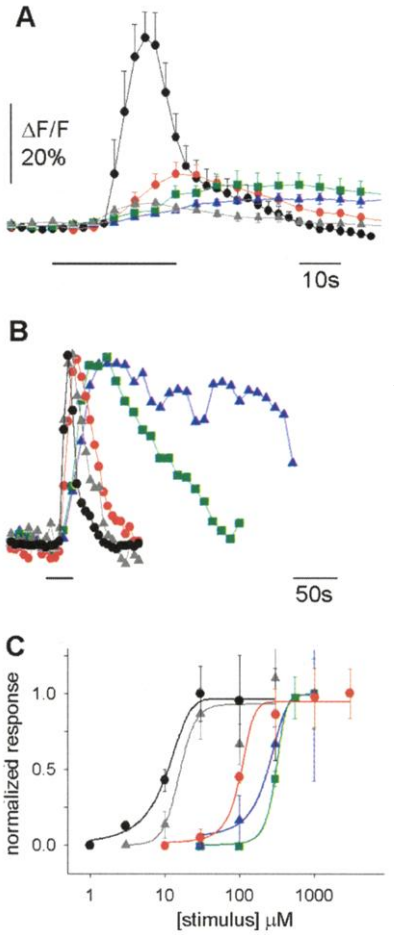

Fig. 3. Ca^{2+} responses elicited by five representative bitter compounds in cell bodies of single taste cells. (**A**) Averaged responses (mean ± SEM, shown by error bars) evoked by cycloheximide (10 μM; n = 10 cells) (black), quinine (300 μM; n = 7) (red), denatonium (100 μM; n = 9) (gray), PTC (300 μM; n = 7) (blue), and SOA (500 μM; n = 6) (green). (**B**) Responses as in (A), but with normalized amplitudes. (**C**) Concentration-response relations show different sensitivities for the five stimuli. Responses are from at least three taste cells. Responses were normalized to the means of the largest responses. Data were curve-fitted as described in Fig. 2F. Error bars indicate SEM. Bars under traces in (A) and (B) denote application of taste stimuli.

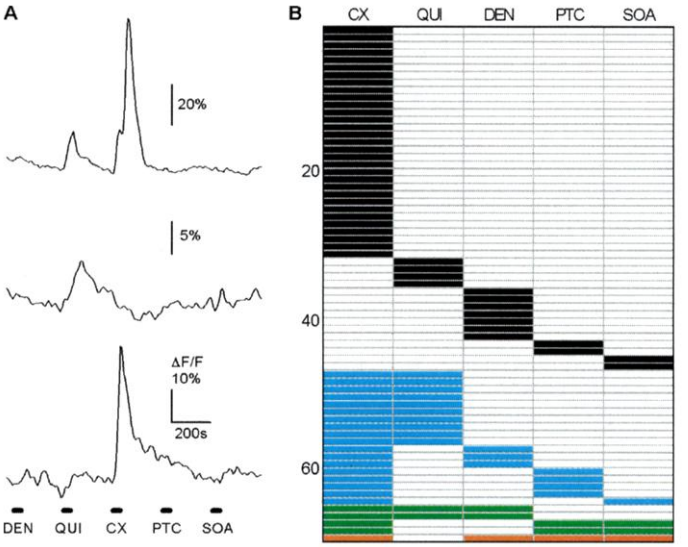

Fig. 4. Chemical specificity of taste cells. (**A**) Sequential stimulation with five bitter stimuli induced different responses in three different taste cells in one taste bud. One cell responded to quinine (300 μM) and cycloheximide (10 μM) (top), one cell responded only to quinine (middle), and one cell responded only to cycloheximide (bottom). (**B**) Summary of the response profiles of 69 bitter-sensitive taste cells (out of 374 imaged cells) as shown in (A). Each column indicates responses to a different bitter compound. Each row represents data from an individual taste cell. The number of cells is indicated on the left. Most taste cells responded to only one stimulus of the five tested (black). Other taste cells responded to two (blue), three (green), and four stimuli (red).

that we tested (18%). Thus, there was no clustering of responses in particular taste buds. The proportion (18%) and spatial pattern of the bitter-sensitive taste cells that we observed within the foliate papillae were similar to those reported for bitter receptor mRNAs [15 to 20% (*1*)].

We next asked whether individual taste receptor cells could discriminate among the five bitter stimuli tested. Stimuli were applied consecutively, in random order that varied from experiment to experiment. Most bitter-sensitive cells (65%, 45 out of 69) responded to only one compound of the five tested, even though neighboring cells responded to other test stimuli (Fig. 4). Twenty-six percent (18 out of 69) of the cells responded to two stimuli, and only 7% (5 out of 69) responded to more than two stimuli. Multiple pairwise comparisons (Fisher's exact test, $P < 0.005$ to keep the overall risk of type I error equal to 0.05) showed that all responses were independent of each other; i.e., there was no association between any two stimuli in taste cells. Applying higher concentrations of denatonium (1 mM) and quinine (1 mM) did not recruit more taste cells (n = 134 taste cells; 5.2 versus 3.7% for denatonium responses at 1 mM and 100 μM, respectively; 4.5 versus 4.5% for quinine responses at 1 mM and 300 μM, respectively). Furthermore, higher concentrations of bitter stimuli did not increase the overlap of responses.

Our results argue against the suggestion that bitter-sensitive taste cells respond to a wide range of bitter stimuli. Instead, our findings indicate that most taste cells may be activated by a limited number of bitter compounds; i.e., individual taste cells can discriminate among bitter stimuli. The specificity of taste cells to bitter stimuli shown in the present study may give rise to the reported segregation of bitter responses into different gustatory nerve fibers (*7*). The existence and nature of any grouping of taste cells were not evident in the present study, but the number of test stimuli (n = 5) was small. Finally, it has yet to be established rigorously whether bitter compounds can be discriminated behaviorally. Human studies (*29*) suggest that there are different categories of bitterness, but the mechanism for this discrimination is not known. Results from nerve recordings and our findings on taste cells support the notion that bitter sensation does not occur through the activation of a single, homogeneous population of bitter-sensitive taste cells, but occurs through the activation of multiple, heterogeneous taste cells.

References and Notes

1. E. Adler *et al.*, *Cell* **100**, 693 (2000).
2. H. Matsunami, J.-P. Montmayeur, L. B. Buck, *Nature* **404**, 601 (2000).
3. J. Chandrashekar *et al.*, *Cell* **100**, 703 (2000).
4. C. Pfaffmann, in *Handbook of Physiology, Section 1, Neurophysiology*, J. Field, Ed. (American Physiological Society, Washington, DC, 1959), vol. 1, pp. 507–533.
5. D. H. McBurney, D. V. Smith, T. R. Shick, *Percept. Psychophys.* **11**, 228 (1972).
6. L. M. Bartoshuk, C. T. Cleveland, *Sens. Processes* **1**, 177 (1977).
7. M. Dahl, R. P. Erickson, S. A. Simon, *Brain Res.* **756**, 22 (1997).
8. T. R. Scott, B. A. Giza, J. Yan, *J. Neurophysiol.* **81**, 60 (1999).
9. A. Caicedo, M. S. Jafri, S. D. Roper, *J. Neurosci.* **20**, 7978 (2000). Tongues were removed from 46 Sprague-Dawley rats (150 to 200 g) and immersed in cold Tyrode's solution [135 mM NaCl, 5 mM KCl, 8 mM $CaCl_2$, 1 mM $MgCl_2$, 10 mM Hepes, 10 mM glucose, 10 mM Na pyruvate, and 5 mM $NaHCO_3$ (pH 7.4, 320 to 330 milliosmol)]. Calcium Green-1 dextran (CaGD) [MW 3000, dissociation constant K_d = 259 nM (Molecular Probes, Eugene, OR)] was injected iontophoretically (5 mM in H_2O; –3.5 μA; 10 min) through a glass micropipette (20-μm tip) into the foliate papillae. Next, the tongues were sliced (100 μm) on a Vibroslicer (Campden Instruments, Leicester, UK). CaGD-loaded cells were excited at 488 nm by using an argon laser attached to an Olympus Fluoview scanning confocal microscope. Confocal images were collected at 5-s intervals, and changes in CaGD fluorescence over time were then analyzed with Fluoview software. We expressed the fluorometric signals as relative fluorescence change, $\Delta F/F = (F - F_0)/F_0$, where F_0 is the resting fluorescence level. All chemicals were applied in a bath at room temperature.
10. Data are most likely recorded from mature receptor cells (*9*). Similar procedures labeled afferent innervation to taste bud cells [R. F. Krimm, D. L. Hill, *J. Comp. Neurol.* **398**, 13 (1998); M. C. Whitehead, J. R. Ganchrow, D. Ganchrow, B. Yao, *Neuroscience* **93**, 931 (1998)]. This also supports the idea that ionto-

phoretically labeled cells are mature (innervated) receptor cells. Furthermore, the incidence of bitter-responsive dye-labeled cells (18%) is remarkably close to the incidence of cells expressing candidate bitter receptors [15 to 20% (*1*)], suggesting that dye-labeled cells are representative taste receptor cells.

11. Ca^{2+} signals presumably indicate physiological activation and presage neurotransmitter release. However, the absence of Ca^{2+} signals does not necessarily indicate that the cell has not been affected (for example, if a stimulus inhibits the taste cell).
12. C. P. Richter, K. H. Clisby, *Am. J. Physiol.* **134**, 157 (1941).
13. H. D. Patton, T. C. Ruch, *J. Comp. Psychol.* **37**, 35 (1944).
14. S. D. Koh, P. Teitelbaum, *J. Comp. Physiol. Psychol.* **54**, 223 (1961).
15. E. Tobach, J. S. Bellin, D. K. Das, *Behav. Genet.* **4**, 405 (1974).
16. K. Iwasaki, M. Sato, *Chem. Senses* **6**, 119 (1981).
17. J. I. Glendinning, *Physiol. Behav.* **56**, 1217 (1994).
18. A. K. Thaw, *Chem. Senses* **21**, 189 (1996).
19. N. K. Dess, *Physiol. Behav.* **69**, 247 (2000).
20. Bath application of cycloheximide (0.1 to 300 μM), denatonium benzoate (3 to 3000 μM), quinine HCl (10 to 3000 μM), SOA (10 to 1000 μM), and PTC (10 to 1000 μM) induced transient Ca^{2+} responses in taste cells in 83% of foliate taste buds tested (43 out of 52 taste buds). At the concentrations used, none of the compounds interfered with fluorescence intensity.
21. Lowering extracellular Ca^{2+} appeared to increase intracellular Ca^{2+} transiently in many cells (Fig. 2D), consistent with previous findings in catfish taste cells [M. M. Zviman, D. Restrepo, J. H. Teeter, *J. Membr. Biol.* **149**, 81 (1996)].
22. Quinine- and denatonium-responsive taste cells (n = 2 for each) also did not show Ca^{2+} increases when depolarized by 50 mM KCl [see also (*25*)].
23. P. M. Hwang, A. Verma, D. S. Bredt, S. H. Snyder, *Proc. Natl. Acad. Sci. U.S.A.* **87**, 7395 (1990).
24. A. I. Spielman *et al.*, *Am. J. Physiol.* **270**, 926 (1996).
25. M. H. Akabas, J. Dodd, Q. Al-Awqati, *Science* **242**, 1047 (1988).
26. T. Ogura, A. Mackay-Sim, S. C. Kinnamon, *J. Neurosci.* **17**, 3580 (1997).
27. The response thresholds versus the behavioral thresholds, respectively, were as follows: 0.1 to 0.3 μM (Fig. 2F) versus 0.2 to 2 μM for cycloheximide (*15*); 10 to 30 μM (red circles, Fig. 3C) versus 8 to 20 μM for quinine (*13*, *14*, *17*, *18*); 3 to 10 μM (gray triangles, Fig. 3C) versus ~1 μM for denatonium (*16*, *17*); 100 to 300 μM (blue triangles, Fig. 3C) versus 20 to 600 μM for PTC (*12*, *15*); and 30 to 100 μM (green squares, Fig. 3C) versus 100 to 200 μM for SOA (*19*).
28. S. Bernhardt, M. Naim, U. Zehavi, B. Lindemann, *J. Physiol.* **490**, 325 (1996).
29. J. F. Delwiche, Z. Buletic, P. A. S. Breslin, paper presented at the XII International Symposium on Olfaction and Taste/XIV Biennial Congress of the European Chemoreception Research Organisation, Brighton, UK, 20 to 24 July 2000.
30. T. Leinders-Zufall, G. M. Shepherd, C. A. Greer, F. Zufall, *J. Neurosci.* **18**, 5630 (1998).
31. This work was supported by NIH grants DC00374 (S.D.R.) and DC04525-01 (A.C.) from the National Institute on Deafness and Other Communication Disorders.

17 October 2000; accepted 22 January 2001

Modulation of Oscillatory Neuronal Synchronization by Selective Visual Attention

Pascal Fries,[1*] John H. Reynolds,[1,2] Alan E. Rorie,[1] Robert Desimone[1]

In crowded visual scenes, attention is needed to select relevant stimuli. To study the underlying mechanisms, we recorded neurons in cortical area V4 while macaque monkeys attended to behaviorally relevant stimuli and ignored distracters. Neurons activated by the attended stimulus showed increased gamma-frequency (35 to 90 hertz) synchronization but reduced low-frequency (<17 hertz) synchronization compared with neurons at nearby V4 sites activated by distracters. Because postsynaptic integration times are short, these localized changes in synchronization may serve to amplify behaviorally relevant signals in the cortex.

Visual scenes typically contain multiple stimuli competing for control over behavior, and attention biases this competition in favor of the most relevant stimulus (*1*). Correspondingly, if two competing stimuli are contained within the receptive field (RF) of an extrastriate neuron, and one of them is attended, the neuron responds as though only the attended stimulus is present (*2*–*6*). Thus, inputs from attended stimuli must have an advantage over inputs from unattended stimuli (*6*). This is apparently not always achieved by a simple increase in firing rates to an attended stimulus, however, because firing rates to a single, high-contrast stimulus in the RF are often not increased with attention (*2*, *5*, *7*). As an alternative to increases in firing rate, one potential "amplifier" of selected neural signals is gamma-frequency synchronization (*8*–*17*). Small changes in gamma-frequency synchronization with attention might lead to pronounced firing-rate changes at subsequent stages (*10*, *18*). Indeed, it was recently reported that neurons in monkey somatosensory cortex showed stronger synchronization during a tactile task than during a visual task, which was presumably caused by increased attention to the tactile stimulus in the tactile task (*19*). However, it is not clear whether the enhanced synchronization was present throughout the somatosensory system or whether it was restricted to those neurons processing the relevant tactile stimuli. To be useful in selective visual attention, enhanced synchronization would need to be confined to neurons activated by the features of attended stimuli, sparing neurons activated by distracters.

We recorded both spikes from small clusters of neurons (multi-unit activity) and local field potentials (LFPs) simultaneously from multiple V4 sites with overlapping receptive fields (RFs) (*20*). The monkey fixated a central spot, and after a short delay, two stimuli were presented at equal eccentricity, one inside and one outside the RFs (Fig. 1C). On separate trials, the monkey's attention was directed to either stimulus location (*21*), and we compared neuronal activity between the two attention conditions. We refer to the condition with attention into the RF as "with attention," always implicitly comparing with identical sensory conditions but with attention outside the RF.

One example pair of recording sites is shown in Fig. 1. The response histograms (Fig. 1D) show stimulus-evoked responses but no clear effect of attention, either during the prestimulus delay or during the stimulus period. To examine the effect of attention on synchronization, we calculated spike-triggered averages (STAs) of the LFP (*11*, *14*, *22*). The STAs revealed oscillatory synchronization between spikes and LFP from two separate electrodes, both during the delay (Fig. 1, E and F) and the stimulus period (Fig. 1, H and I). During the delay, the power spectra of the STAs (Fig. 1G) were dominated by frequencies below 17 Hz. With attention, this low-frequency synchronization was reduced (*23*). During the stimulus period, there were two distinct bands in the power spectrum of the STAs (Fig. 1J), one below 10 Hz and another at 35 to 60 Hz. With attention, the reduction in low-frequency synchronization was maintained and, conversely, gamma-frequency synchronization was increased.

To determine whether these changes in synchronization were precisely localized within V4, we made additional recordings with the stimulus outside the RF very close to the RF border (Fig. 2). Even with closely spaced stimuli, we found the same attentional modulation of synchronization as with the second stimulus far away (Fig. 2, C to E). In

[1]Laboratory of Neuropsychology, National Institute of Mental Health, National Institutes of Health, Building 49, Room 1B80, 9000 Rockville Pike, Bethesda, MD 20892–4415, USA. [2]Systems Neurobiology Laboratory, The Salk Institute for Biological Studies, 10010 North Torrey Pines Road, La Jolla, CA 92037–1099, USA.

*To whom correspondence should be addressed. E-mail: fries@ln.nimh.nih.gov